Dalton Transactions

An international journal of inorganic chemistry

Accepted Manuscript

This article can be cited before page numbers have been issued, to do this please use: J. Rubín, L. Badía-Romano, F. Luis, V. Mereacre, D. Prodius, A. Arauzo, F. Bartolomé and J. Bartolomé, *Dalton Trans.*, 2020, DOI: 10.1039/C9DT04816B.

ROYAL SOCIETY OF CHEMISTRY

rsc.li/dalton

View Article Online
DOI: 10.1039/C9DT04816B

Journal Name

ARTICLE TYPE

Cite this: DOI: 10.1039/xxxxxxxxxx

Magnetic chains of Fe_3 clusters in the $\{Fe_3YO_2\}$ butterfly molecular compound†

Javier Rubín,*[a,b] Laura Badía-Romano,[a,c] Fernando Luis,[a,c] Valeriu Mereacre,[d] Denis Prodius,[d] Ana Arauzo,[c,e] Fernando Bartolomé,[a,c] and Juan Bartolomé[a,c]

Received Date
Accepted Date

DOI: 10.1039/xxxxxxxxxx

www.rsc.org/journalname

The "butterfly" molecule $[Fe_3Y(\mu_3{-}O)_2(CCl_3COO)_8(H_2O)(THF)_3]$ (in brief $\{Fe_3YO_2\}$) includes three Fe^{3+} ions which build a robust Fe_3 cluster with a strong intracluster antiferromagnetic exchange $\mathscr{J}/k_B = -50\,K$ and a total spin $S = 5/2$. It represents the starting magnetic system to study further interactions with magnetic rare earths when Y is replaced with lanthanides. We present heat capacity and equilibrium susceptibility measurements below 2 K, which show that each cluster has a sizeable magnetic anisotropy pointing to the existence of intercluster interactions. However, no phase transition to a long-range magnetically ordered phase is observed down to 20 mK. The intercluster interaction is analysed in the framework of the one-dimensional Blume-Capel model with an antiferromagnetic chain interaction constant $J/k_B = -40(2)$ mK between Fe_3 cluster spins, and a uniaxial anisotropy with parameter $D/k_B = -0.56(3)$ K. This is associated to single chains of Fe_3 clusters oriented along the shortest intercluster distances displayed by the crystal structure of $\{Fe_3YO_2\}$. *Ac* susceptibility measurements reveal that the magnetic relaxation is dominated by a quantum tunnelling process below 0.2 K, and by thermally activated processes above this temperature. The experimental activation energy of this single chain magnet, $E_a/k_B = 3.4(6)$ K, can be accounted for by the combination of contributions arising from single-molecule magnetic anisotropy and spin-spin correlations along the chains.

1 Introduction

Molecular magnets are attracting much attention because of their potential applications as spintronic elements,[1] in quantum information processing[2–6] or in magnetic cooling.[7] Among the plethora of new molecules, the polynuclear magnetic clusters provide a large class of materials which show single molecule magnet (SMM) behaviour, *i.e.*, they show remanence after application of a magnetic field even though there is no significant interaction between neighbouring clusters. However, many of them undergo thermally activated quantum tunneling of magnetization (TAQTM) or pure quantum tunneling of magnetization (QTM) that inhibit the SMM behaviour. The tunneling dynamics is a collective process, as tunneling probabilities depend very strongly on the bias fields generated by the neighbouring spins that change every time one of them flips.[8,9] In spite of this, the effect that magnetic long range order produced by dipolar interactions between magnetic clusters, as has been observed in Mn_{12}-acetate and Fe_8,[10,11] has on magnetic relaxation remains largely unexplored.

A class of clusters of special interest is that of bimetallic clusters, which are constituted by transition metals M that provide most of the cluster magnetization, and rare earth metals Ln that generate an enhanced magnetic anisotropy *via* intracluster interactions.[13,14] Within this class of $\{M_xLn_y\}$ clusters, the molecules $[Fe_3Ln(\mu_3{-}O)_2(CCl_3COO)_8(H_2O)(THF)_3]$, in brief $\{Fe_3LnO_2\}$, provide a series of isostructural compounds that allows exploring how the magnetic properties vary as a function of the different Ln substitutions.[15] All members of this series have a "butterfly" type $\{Fe_3Ln(\mu_3{-}O)_2\}^{8+}$ core. The three Fe^{3+} ions form a triangle, Fe_3, with the Fe(2) atom (Fig. 1) at the body of the butterfly and the two Fe(1) and Fe(3) atoms at the wings. All Fe ions are in the $S = 5/2$ high spin state and the Fe(1)-Fe(2) and Fe(2)-Fe(3) exchange interactions, $\mathscr{J}$, are antiferromagnetic while that of Fe(1)-Fe(3), $\mathscr{J}'$, is negligible, yielding a total spin $S_T = 5/2$ for the Fe_3 subcluster.[12] The $Fe_3{-}Ln$ intracluster interaction within

[a] *Instituto de Ciencia de Materiales de Aragón, CSIC - Universidad de Zaragoza, E-50018 Zaragoza, Spain. Fax: XX XXXX XXXX; Tel: XX XXXX XXXX; E-mail: xxxx@aaa.bbb.ccc*
[b] *Dept. Ciencia y Tecnología de Materiales y Fluidos, Universidad de Zaragoza, E-50018 Zaragoza, Spain.*
[c] *Dept. Física de la Materia Condensada, Universidad de Zaragoza, E-50009 Zaragoza, Spain.*
[d] *Institute of Chemistry, Academy of Science of Moldova, MD-2028 Chisinau, Republic of Moldova.*
[e] *Servicio de Medidas Físicas, Universidad de Zaragoza. E-50009 Zaragoza, Spain.*
† Electronic Supplementary Information (ESI) available: [details of any supplementary information available should be included here]. See DOI: 10.1039/b000000x/

View Article Online
DOI: 10.1039/C9DT04816B

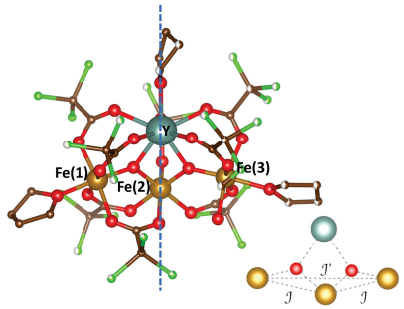

Fig. 1 Structure of $[Fe_3Y(\mu_3{-}O)_2(CCl_3COO)_8(H_2O)(THF)_3]$, the vertical dashed line shows a quasi-symmetry plane of the $\{Fe_3YO_2\}$ core.The $\{Fe_3YO_2\}$ core is sketched in the bottom right corner with the Fe_3 intercluster interactions $\mathscr{J}$ and $\mathscr{J}'$ as defined in [12].

the "butterfly" molecule (for a magnetic Ln lanthanide) is also antiferromagnetic.[12] The intensity of the intracluster interaction was also evaluated in a combined study of conventional magnetometry and x ray magnetic circular dichroism as a function of applied magnetic field, both in the case of Kramers ions as Ln = Gd and Dy[16] and of non-Kramers ions as Ln = Tb and Ho.[17,18]

The goal of the present work is to investigate in detail the interactions and relaxation processes in the absence of a magnetic rare earth, for which the standard choice of Y as a substitution for a non magnetic rare earth is made, since the crystal structure is approximately preserved.[15] Focusing on Fe_3 clusters as magnetic units can help to study and understand the role of intercluster interactions, and it will be shown that those interactions take place along chains. Furthermore, two relaxation processes are revealed at different temperature ranges, which bring out the rôle of intra and intercluster interactions on magnetic relaxation.

The paper is structured as follows: Section 2 describes the experimental techniques and procedures used in the present study. In Section 3, equilibrium heat capacity and magnetic susceptibility data measured down to 20 mK are presented and analysed, in order to search for signatures arising from intercluster interactions. This study shows that such intercluster interactions may be modelled as a single chain magnetic system. Single-molecule and chain correlation relaxation processes are investigated by *ac* magnetic susceptibility in Sec. 4. Finally the results are discussed in Sec. 5.

2 Experimental details

The synthesis of the $[Fe_3Y(\mu_3{-}O)_2(CCl_3COO)_8(H_2O)(THF)_3]$ compound has been reported in previous works.[15,19] The sample was in powder form and its purity was checked by X-ray diffraction. Heat capacity $C(T)$ under different applied magnetic fields $(0-40\,\mathrm{kOe})$ was measured on a powder sample embedded in Apiezon N grease, using a Quantum Design PPMS. Experiments in the low temperature region $(0.35\,\mathrm{K} < T < 10\,\mathrm{K})$ were carried out with the ^{3}He option of the same PPMS, while for temperatures ranging between 2 K and 20 K, the base system was used. The coincident temperature range $(2\,\mathrm{K} < T < 10\,\mathrm{K})$ was intended to scale the low T to the absolute high T measurements. Measurements under zero magnetic field were carried out up to 100 K.

The dynamic behaviour as a function of temperature and magnetic field was studied by means of *ac* susceptibility measurements at varying frequency. Measurements on the present compound were performed, above 1.8 K, using a Quantum Design superconducting quantum interference device (SQUID) magnetometer and the ACMS option of a Quantum Design PPMS to cover a large range of frequency. *Ac* measurements were carried out at an excitation field of 4 Oe, and under *dc* fields between 0 and 10 kOe, while sweeping the frequency in the range 0.1 Hz−1.5 kHz for the SQUID and 100 Hz−10 kHz for the PPMS. The sample was soaked in a Daphne oil drop, introduced to fix the grain orientation at low temperature. Additionally, *ac* susceptibility measurements in the region of very low temperature $(0.018\,\mathrm{K} < T < 3\,\mathrm{K})$ were performed using a microSQUID susceptometer and a Leiden Cryogenics ^{3}He-^{4}He dilution refrigerator. The voltage signal from the susceptometer was converted into magnetic units (emu·mol^{-1}) by scaling with data obtained with the SQUID susceptometer in coincident temperature and frequency.

3 Equilibrium heat capacity and magnetic susceptibility

The molar heat capacity of $\{Fe_3YO_2\}$ measured between 0.3 K and 100 K at zero field is shown in Fig. 2-top. The lattice contribution shows up above $T \approx 5$ K, while below that temperature a magnetic contribution is clearly observed. The shape of $C(T)$ displays a Schottky-type maximum centred at ≈ 0.9 K followed by a dip at around 2 K. The Schottky peak is discussed below, and it reflects that the $S_{Fe3} = 5/2$ multiplet is split by a ligand field effect. Then, the dip provides a temperature range where the $C_{Sch} \approx AT^{-2}$ Schottky peak tail at the high temperature side and the $C_{latt} \approx BT^3$ low temperature dependence of the lattice contribution meet. Therefore, the dip is expected to show a dependence $CT^2 = A + BT^5$, from which B can be obtained.[20] Following this procedure for the $\{Fe_3YO_2\}$ compound, the value $B = 8.42(8) \times 10^{-3}\,\mathrm{K}^{-3}$ was obtained, which yields a Debye temperature of $\theta_D = 157(1)$ K.

In a previous work it has been shown that the magnetic susceptibility and magnetization of the trinuclear iron cluster in $\{Fe_3YO_2\}$ measured above 2 K could be described in terms of the Heisenberg-Dirac-van Vleck (HDVV) model where the three Fe^{3+} ions are antiferromagnetically coupled.[12] The Fe(1)-Fe(2) and Fe(2)-Fe(3) ("body-wing") interaction constant is $\mathscr{J}/k_B = -50$ K, while the Fe(1)-Fe(3) ("wing-wing") coupling is negligible. As a result, the Fe(1,3) spins are oppositely oriented with respect to the Fe(2) one. Therefore, at temperatures below 2 K the Fe_3 cluster can be considered as a unit with $S_{Fe3} = 5/2$.

The zero field splitting (ZFS) of the $S_{Fe3} = 5/2$ ground state,

View Article Online
DOI: 10.1039/C9DT04816B

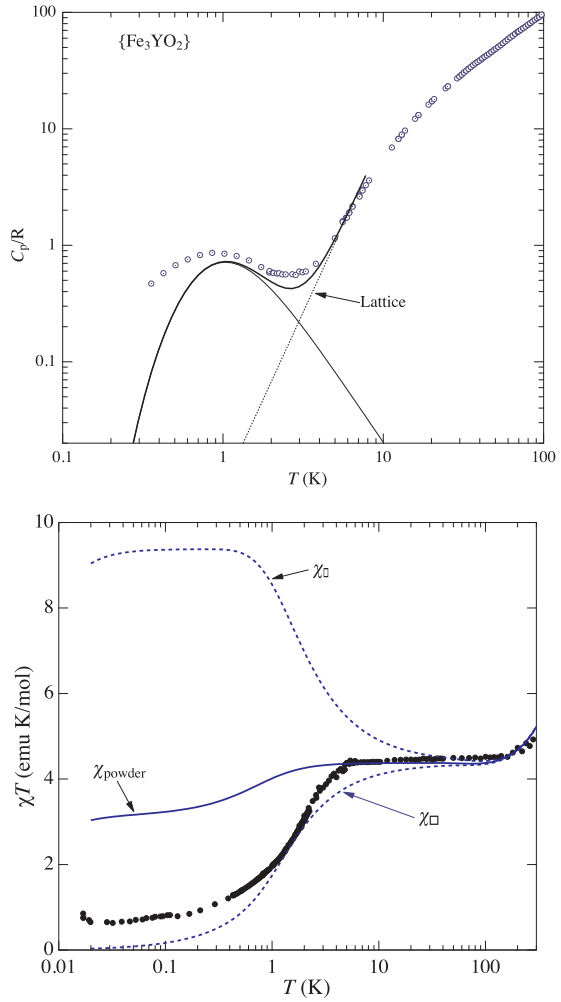

Fig. 2 Top: Heat capacity of $\{Fe_3YO_2\}$ as a function of temperature from 0.35 K to 100 K, along with the estimated lattice contribution $C_{\rm latt}$ (dotted line), the magnetic contribution from the Fe_3 cluster anisotropy $C_{\rm ani}$ (thin full line) and the total heat capacity $C_{\rm latt}+C_{\rm ani}$ for $T<10$ K (thick full line). Bottom: Experimental susceptibility χT, along with the calculation of the parallel, perpendicular and random powder average for Fe_3 clusters with cluster anisotropy $D/k_{\rm B}=-0.56$ K and no intercluster exchange interaction.

which reflects itself in the Schottky anomaly at zero magnetic field, can be accounted for by a uniaxial magnetic anisotropy of the Fe_3 subcluster. The energy levels can be calculated using the spin Hamiltonian:

$$\hat{H}=\hat{H}_{\rm ex}+\hat{H}_{\rm LF} \qquad (1)$$

where $\hat{H}_{\rm ex}$ is the exchange Hamiltonian of the three Fe^{3+} cluster (intracluster interaction) with spins $\vec{S}_1$, $\vec{S}_2$ and $\vec{S}_3$, in the Heisenberg-Dirac-Van Vleck approximation

$$\hat{H}_{\rm ex}=-2\mathscr{J}\left(\vec{S}_1\cdot\vec{S}_2+\vec{S}_2\cdot\vec{S}_3\right)-2\mathscr{J}'\left(\vec{S}_1\cdot\vec{S}_3\right) \qquad (2)$$

and $\hat{H}_{\rm LF}^{\rm Fe_3}$ is the ligand field term acting on the spin-orbit perturbed levels of each individual Fe atom.

At the "butterfly" molecule the three Fe^{3+} ions occupy the centres of similar slightly distorted oxygen octahedra. Therefore the ZFS Hamiltonian can be described with a uniaxial anisotropy with rhombic distortion

$$\hat{H}_{\rm LF}=\sum_{i=1}^{3}\left\{D_i\hat{S}_{z,i}^2+E_i\left(\hat{S}_{x,i}^2-\hat{S}_{y,i}^2\right)\right\} \qquad (3)$$

where D_i are the uniaxial anisotropy constants and E_i the rhombocity parameters of each Fe ion i. Assuming that the three Fe^{3+} ions have ligand fields with uniaxial symmetry that imposes a common alignment direction, the ligand field term simplifies to

$$\hat{H}_{\rm LF}=D\hat{S}_{\rm z,Fe3}^2+E\left(\hat{S}_{\rm x,Fe3}^2-\hat{S}_{\rm y,Fe3}^2\right) \qquad (4)$$

since it can be proved that in the strong exchange limit the cluster anisotropy Hamiltonian in terms of the individual spins S_i can be expressed as an effective ZFS Hamiltonian of the total spin $S_{\rm Fe3}$.[21] This approximation is valid provided that $|\mathscr{J}|\gg D_i$, which is fulfilled in $\{Fe_3YO_2\}$ (*vide infra*), since $\mathscr{J}/k_{\rm B}=-50$ K.[12] The rhombocity parameter E amounts to a second-order correction in E/D to the main uniaxial anisotropy.

The magnetic heat capacity was simulated from the energy eigenvalues of the Hamiltonian (1) using the code MAGPACK,[22] and the values of intracluster exchange constants $\mathscr{J}/k_{\rm B}=-50$ K and $\mathscr{J}'=0$ found previously.[12] The temperature of the broad specific heat maximum observed below 2 K can be accounted for with an uniaxial anisotropy constant $D/k_{\rm B}=-0.56(3)$ K, which is much smaller than $\mathscr{J}$. The contribution of the intracluster Fe-Fe interactions to the heat capacity is negligible in this temperature range. However, the magnetic anisotropy cannot account, by itself, for the width of the Schottky anomaly and, in particular, for the excess in specific heat observed below 1 K, irrespective of the value of rhombic distortion parameter E.

The magnetic entropy change was calculated by integration of $C_{\rm m}(T)/T=(C-C_{\rm latt})/T$ in the temperature range from 0.35 K to 5 K and by extrapolation of the $C_{\rm m}(T)$ data to a T^{-2} law from 5 K to ∞, yielding to a value $\Delta S_{\rm m}^{\rm exp}/R=1.56(2)$. The $S=5/2$ ground sextuplet is split by the anisotropy field yielding to a groundstate doublet with $S_z=\pm5/2$, and two excited doublets $S_z=\pm3/2$ and $S_z=\pm1/2$ which are $4|D|/k_{\rm B}=2.24$ K and $6|D|/k_{\rm B}=3.36$ K higher in energy, respectively. This can only produce an entropy change of $\Delta S_{\rm m}/R=\ln 3=1.10$. The next excited multiplet of the Fe_3 cluster lays at ≈ 250 K from the ground state and therefore it cannot contribute to ΔS in the low temperature range.

The excess of heat capacity observed below ≈ 2 K, hence the excess of entropy, can only be produced by additional degrees of freedom. These could be provided by interactions between Fe_3 clusters that can split the otherwise degenerate spin doublets even at zero external field. The heat capacity measurements down to $T=0.35$ K(Fig. 2-top), and the equilibrium susceptibility measurements to $T=18$ mK show no signature of a phase transition to a long-range magnetically ordered state (Fig. 2-bottom). Therefore 2-dimensional (2D) or 3D interactions between Fe_3 clusters are expected to be negligible. Indeed, we perfomed numerical calculations of the heat capacity using a a 2D rectangular Ising model,[23] which show that the ratio of the two perpendicular interaction constants should be higher than 100 in order to exclude effects of a transition in the heat capacity in the experimental

View Article Online
DOI: 10.1039/C9DT04816B

temperature range. Therefore we conclude that the intercluster interactions must predominantly be of 1D character.

The need for an intercluster interaction in addition to the intracluster ligand field can also be inferred from the low frequency magnetic susceptibility data measured with the SQUID ($1.8 < T < 250\,\mathrm{K}$, $f = 10\,\mathrm{Hz}$) and microSQUID ($16\,\mathrm{mK} < T < 2\,\mathrm{K}$, $f = 1.6\,\mathrm{Hz}$) magnetometers and plotted as $\chi(T)T$ in Fig. 2-bottom. This low frequency susceptibility will be taken as the equilibrium susceptibility as it will be justified in Sec. 4. Below $\approx 200\,\mathrm{K}$ and down to $\approx 5\,\mathrm{K}$, χT remains approximately constant. This Curie-Weiss behaviour ($\chi = \mathscr{C}/(T-\theta)$) in this temperature range yields $\mathscr{C} = 4.52(1)\,\mathrm{emu\,K/mol}$ and $\theta = -0.27(4)\,\mathrm{K}$, in agreement with a previous determination.[15] This shows the paramagnetic behaviour of $S = 5/2$ spins with all their levels being thermally populated (the highest level for the cluster spin is $6D/k_\mathrm{B} = 3.36\,\mathrm{K}$ above the ground state level $S_z = \pm 5/2$), which predicts a Curie constant $\mathscr{C} = 4.375\,\mathrm{emu\,K/mol}$, and points to the existence of an antiferromagnetic coupling between the Fe_3 clusters. As temperature decreases, a downturn to a plateau develops, with an inflection point at $T \approx 1.8\,\mathrm{K}$, which is caused by the thermal depopulation of the $S = 5/2$ sextuplet split by the ligand field anisotropy.

The calculated χT, with $D/k_\mathrm{B} = -0.56\,\mathrm{K}$, intracluster exchange constants $\mathscr{J}/k_\mathrm{B} = -50\,\mathrm{K}$ and $\mathscr{J}' = 0$, and no intermolecular interactions, is also shown in Fig. 2-bottom for $\vec{H}$ parallel ($\chi_\parallel$) and perpendicular ($\chi_\perp$) to the anisotropy axis and for a random powder $\chi_\mathrm{powder} = (1/3)\chi_\parallel + (2/3)\chi_\perp$. The upturn in χT for temperatures above $\approx 150\,\mathrm{K}$ is well reproduced. The effect of a small Fe(1)-Fe(3) interaction was also explored; it only shows up in the high temperature upturn reflecting the change from the paramagnetic susceptibility of the $S = 5/2$ Fe_3 clusters to the paramagnetic susceptibility of the $S_i = 5/2$ Fe^{3+} individual ions, but no effect is found at low temperature. The calculated decrease to a low temperature plateau is in qualitative agreement with experiment, but the predicted low temperature χT value is at least two times larger than the experimental one below 1 K. The discrepancy might be due to defective random orientation of grains placed in the microSQUID sensitive area, but then the experimental result should also lay below χ_powder in the $5 - 10\,\mathrm{K}$ range.

In order to account for the experimental heat capacity including 1D intercluster interactions, a 1D Ising model with spin-S in the presence of a uniaxial crystal field[24] (a generalization of the original $S = 1$ Blume-Capel model[25]) will be used (see ESI†). The model has been worked out using the transfer matrix method.[24,26] The calculations for $S \geq 3/2$ can be perfomed numerically, what we have done for the case of an antiferromagnetic chain of $S = 5/2$ spins with uniaxial anisotropy from the Hamiltonian

$$\hat{H}_\mathrm{C} = -2J \sum_{i=1}^{N} S_{z,i} S_{z,i+1} + D \sum_{i=1}^{N} S_{z,i}^2 \qquad (5)$$

starting from a ring of N spins with periodic boundary conditions $S_{z,N+1} = S_{z,1}$, and then taking the thermodynamic limit $N \to \infty$.

Fig. 3 shows that an interaction constant of $J/k_\mathrm{B} = -40\,\mathrm{mK}$, in addition to an uniaxial anisotropy parameter $D/k_\mathrm{B} = -0.56\,\mathrm{K}$ accounts fairly well for the experimental heat capacity all over

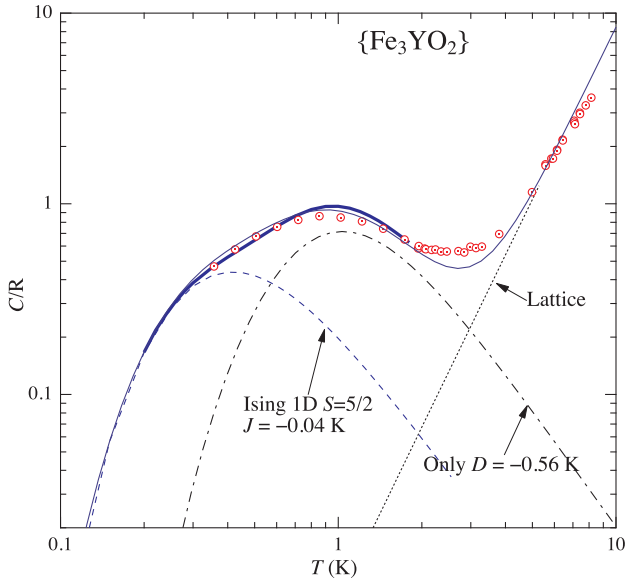

Fig. 3 Experimental heat capacity of the $\{Fe_3YO_2\}$ compound (circles) and calculated heat capacity for: (a) Infinite chain in the Blume-Capel model with $J/k_\mathrm{B} = -40\,\mathrm{mK}$, $D/k_\mathrm{B} = -0.56\,\mathrm{K}$ (thick full line), (b) Only intracluster ligand field anisotropy (dashed-dotted line), (c) Only chain intercluster interaction with $J/k_\mathrm{B} = -40\,\mathrm{mK}$ (dashed line), and (d) Addition of (b) and (c) (thin full line). For the total heat capacities of (a) and (d), the lattice contribution was added.

the accessible temperature range. The interaction constant J proves to be an order the magnitude smaller than the intracluster anisotropy parameter. In fact, the addition of the contributions to the heat capacity arising from the anisotropy of the clusters as calculated from Eq. 4 on one side, and from an Ising model of $S = 5/2$ spins interacting along 1D on the other side, taken both as independent of each other, closely reproduces the full calculation performed using the Blume-Capel model (compare curves (a) and (d) in Fig. 3). The entropy change in the Ising linear chain amounts to $R\ln 2$, to be added to the ZFS entropy of $R\ln 3$. The total entropy of $R\ln 6 \approx 1.79R$ is to be compared to the experimental $\Delta S_\mathrm{m}^\mathrm{exp} = 1.56(2)R$ for temperatures above 0.35 K.

Additional measurements of C_p under external magnetic fields are shown in the Supplemental Information along with Monte Carlo simulations.† The above proposed model of a clusters chain with $D/k_\mathrm{B} = -0.56\,\mathrm{K}$ and $J/k_\mathrm{B} = 40\,\mathrm{mK}$ also reproduces the experimental specific heat when a external field is applied.

The same type of calculation for the powder averaged magnetic susceptibility is not so straightforward. The parallel susceptibility can be easily calculated analytically for $S \leq 3/2$,[24,26] while for $S > 3/2$ numerical calculations can be performed.[26] Using the method described by Chatterjee,[26] $\chi_\parallel T$ for $S = 5/2$ was calculated for the values $J/k_\mathrm{B} = -40\,\mathrm{mK}$ and $D/k_\mathrm{B} = -0.56\,\mathrm{K}$ obtained from the heat capacity. It shows a maximum at $\approx 3\,\mathrm{K}$ and a drop to zero as temperature decreases. In contrast, the perpendicular susceptibility in the Blume-Capel model is a much more difficult task.[27] The perpendicular susceptibility $\chi_\perp T$ is expected to behave in a similar way without a maximum, as shown by the calculation for the case in which only the magnetic anisotropy is present (Fig.

View Article Online
DOI: 10.1039/C9DT04816B

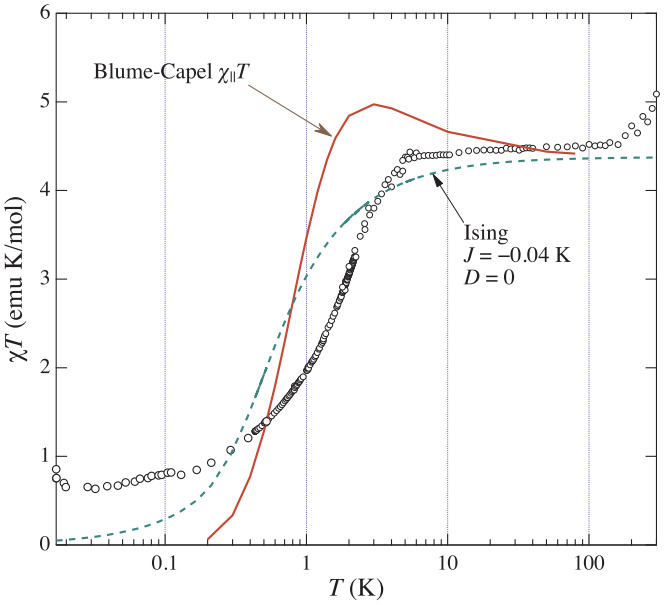

Fig. 4 Experimental (large circles) and calculated χT of the $\{Fe_3YO_2\}$ compound for: (a) Parallel χT using a Blume-Capel model for an antiferromagnetic chain with $J/k_B = -40$ mK and $D/k_B = -0.56$ K and (b) Ising antiferromagnetic chain with $J/k_B = -40$ mK.

2-bottom).

Alternatively, we have approached the calculation of the powder averaged susceptibility in a different way. On the one hand, the 1D Ising, and the 1D Heisenberg susceptibility were calculated (see ESI†). The temperature dependence qualitatively describes the experimental results, but obviously it does not account for the non-zero value of χT that is observed at the lowest temperatures. On the other hand, both $\chi_{\|}T$ and $\chi_{\perp}T$ were calculated with a constrained Monte Carlo simulation of a Heisenberg linear chain of classical spins using the code VAMPIRE.[28] None of the calculations reproduce completely the experimental susceptibility, but they definitely show that antiferromagnetic intercluster interactions have to be taken into account in order to account for the experimental results.

4 Magnetic relaxation

The spin dynamics of $\{Fe_3YO_2\}$ was explored by *ac* magnetic susceptibility as a function of frequency, temperature and external magnetic field H. The in-phase, $\chi'(T)$, and out-of-phase, $\chi''(T)$, curves measured for $H = 0$ display a frequency dependence (see Fig. 5), but only at very low temperatures, with $\chi''(T)$ increasing for increasing frequency, which reveals a relaxation process. Although at the lowest temperatures (Fig. 5 insets) no maximum in $\chi''(f)$ shows up, an estimation of the relaxation time can be obtained from the expression

$$\tau \approx \frac{\chi''(T,f)}{2\pi f\,(\chi'(T,f) - \chi_{ad})} \qquad (6)$$

where χ_{ad} is the adiabatic, or infinite frequency, limit susceptibility. Since the limited frequency of our experimental window did not allow us to measure χ_{ad}, we will assume the approximation $\chi_{ad} = 0$ in that temperature range. The relaxation time is very short ($\tau_f \approx 3 \times 10^{-7}$ s) and temperature independent within experimental errors (Fig. 6). We ascribe this process to quantum tunneling of the magnetization (QTM) of the cluster's magnetic moment through the anisotropy barrier between the two states of the $S^z_{Fe3} = \pm 5/2$ ground Kramers doublet. Since time-reversal symmetry forbids tunneling for half-odd spin systems ("van Vleck cancellation"[29,30]), this process would here be driven by an internal transversal magnetic field. At $H = 0$ applied field such a fast relaxation process allows the spin system to reach thermal equilibrium within the time scales of the heat capacity and low frequency *ac* susceptibility measurements (Fig. 2), and to establish 1D spin correlations.

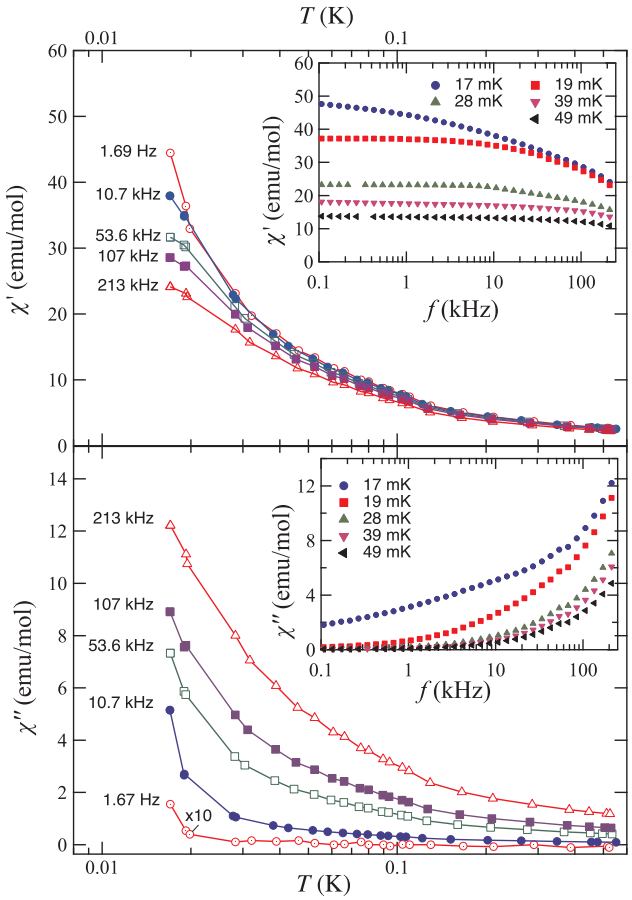

Fig. 5 Very low temperature ac susceptibility of $\{Fe_3YO_2\}$ as a function of temperature, in the frequency range $1.6\,\text{Hz} < f < 213\,\text{kHz}$. Upper panel: $\chi'(T)$. Lower panel: $\chi''(T)$. Frequency dependence at the lowest measured temperatures in the insets.

For higher temperatures, the zero-field *ac* susceptibility χ'' becomes very small. Possible relaxation processes can be made apparent under the application of an external *dc* magnetic field, which will rapidly suppress QTM as a side effect. Indeed, as the applied field increases ($0 < H \leq 30$ kOe), the $\chi''(f)$ curves show rounded maxima of increasing amplitude up to a certain value of H (see ESI†). In order to have a good signal of $\chi'(f)$ and $\chi''(f)$ for

View Article Online
DOI: 10.1039/C9DT04816B

temperatures above 1 K, $H = 6.5$ kOe was chosen for the measurements of *ac* susceptibility at frequencies in the $0.1 < f < 10^4$ Hz range. The data are included in Fig. 7 for temperatures from 1.8 K to 5 K.

The $\chi''(f)$ curves show three main features:

i. A low frequency maximum at $f \approx 0.4$ Hz, which reveals the existence of a very slow relaxation process. The relaxation time of this process, τ_s, has been estimated either from the position of the maxima in $\chi''(f)$ at each temperature or from the maxima in Cole-Cole diagrams ($\chi''(\chi')$). The height of the maximum increases with decreasing temperature.

ii. An increase in $\chi''(f)$ at frequencies higher than 1 kHz pointing to a maximum lying outside or in the limit of the experimental frequency range, which reveals some remaining "fast" processes ($\sim 10^{-5}$ s). The intensity of this component decreases with decreasing temperature, *i.e.*, behaves in an opposite way to that of the slow processes.

iii. Non negligible values in the intermediate frequency range $10 - 100$ Hz. This points to the existence of a third relaxation process with characteristic time scales intermediate between those of the "fast" and "slow" processes.

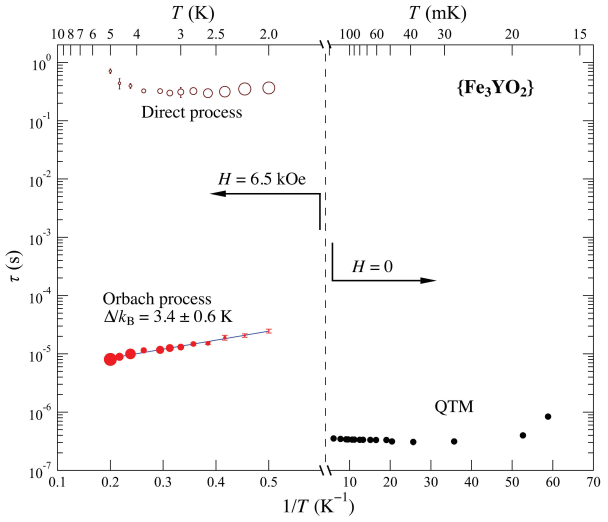

Fig. 6 Low temperature relaxation times τ *versus* temperature. Right half: From χ_{ac} with no *dc* magnetic field (Fig. 5) and Eq. 6. Left half: From χ_{ac} with applied *dc* magnetic field $H = 6.5$ kOe (Fig. 7) and Eq. 8. The size of the open circles denote the evolution with temperature of the relative intensity of each component.

In order to extract information from the $\chi''(\omega)$ curves, we considered $\chi(\omega) = \chi'(\omega) - i\chi''(\omega)$, with $\omega = 2\pi f$ as made of three components $\chi(\omega) = \chi_d(\omega) + \chi_{in}(\omega) + \chi_{or}(or)$, where the subscript "d", "in" and "or" correspond to the slow, intermediate and fast processes, respectively. Each component was modelled as an independent generalized Debye process[31]

$$\chi(\omega) = \chi_{ad} + \sum_v \frac{\chi_{T,v} - \chi_{ad}}{1 + (i\omega\tau_v)^{1-\alpha_v}} \qquad (7)$$

where χ_T is the isothermal susceptibility and $v = $ d, in, or. The slow and fast components were considered as single-process type susceptibilities, *i.e.*, $\alpha_d = \alpha_{or} = 0$, while the intermediate component was assumed to include a distribution of processes to account for the susceptibility in the intermediate frequency range. The in-phase and out-of-phase components of the susceptibility

$$\chi'(\omega) = \chi_{ad} + \sum_v a_v \frac{1 + \sin(\alpha_v\pi/2)(\omega\tau_v)^{1-\alpha_v}}{1 + (\omega\tau_v)^{2-2\alpha_v} + 2\sin(\alpha_v\pi/2)(\omega\tau_v)^{1-\alpha_v}}$$

$$\chi''(\omega) = \sum_v a_v \frac{\cos(\alpha_v\pi/2)(\omega\tau_v)^{1-\alpha_v}}{1 + (\omega\tau_v)^{2-2\alpha_v} + 2\sin(\alpha_v\pi/2)(\omega\tau_v)^{1-\alpha_v}} \qquad (8)$$

were fitted simultaneously for each temperature. The values of $\tau_d(T)$ and $\tau_{or}(T)$ are shown in Fig. 6. The distribution for the intermediate process shows values of $\alpha_{in} \approx 0.5$, except for $T > 4$ K where it increases up to ≈ 0.8, and its intensity shows a similar temperature dependence to that found for the slow process component all over the temperature range.

The relaxation time of the slow process is almost temperature independent with $\tau_d \approx 0.4$ s and its intensity increases as temperature decreases (Fig. 6). Such a slow relaxation time is very similar to those observed in Ln=Dy and Tb polymeric chains that we have studied earlier.[32–35] Its value was shown to depend strongly on the He gas pressure of the SQUID sample chamber, *i.e.*, when the chamber is vented or purged, which modifies the thermal contact between the sample and the cold bath.[35] This behaviour is indicative of a phonon-bottleneck effect which may increase by several orders of magnitude the measured relaxation time of direct processes at low temperature, where the lattice heat capacity is very low with respect to the magnetic contribution.[35] The intensity of the component in the intermediate frequency range shows a similar behaviour to that of the slow process: an almost temperature independent relaxation time ≈ 0.05 s, and increasing intensity with decreasing temperature.

The "fast" relaxation time turns out to be temperature dependent (Fig. 6) and it could be fitted using an Arrhenius law with $\tau_0 = 4.4 \times 10^{-6}$ s and activation energy $E_a/k_B = 3.4(6)$ K. Since under an external applied field the tunneling process is quenched, the observed relaxation is a thermally activated process over an anisotropy barrier with possible contributions of the spin chain correlations.

5 Discussion

The "butterfly" Fe_3 cluster shows identical exchange interaction between each Fe(1) and Fe(3)"wing" Fe(III) ions and the Fe(2) "body" ion and negligible interaction between the "wing" ions. Therefore, magnetically it constitutes a symmetric linear triad.[36] In the strong exchange limit the individual anisotropy constants D_i can be related to the effective anisotropy constant D of the Fe_3 cluster. Following the procedure described in Bencini & Gatteschi[36] the relationship $D = 1.595 D_i$ was obtained. The value $D_i/k_B = -0.35$ K from the present heat capacity measurements is negative and with absolute value less than half or similar of those reported for high spin Fe(III) in single-ion compounds from

View Article Online
DOI: 10.1039/C9DT04816B

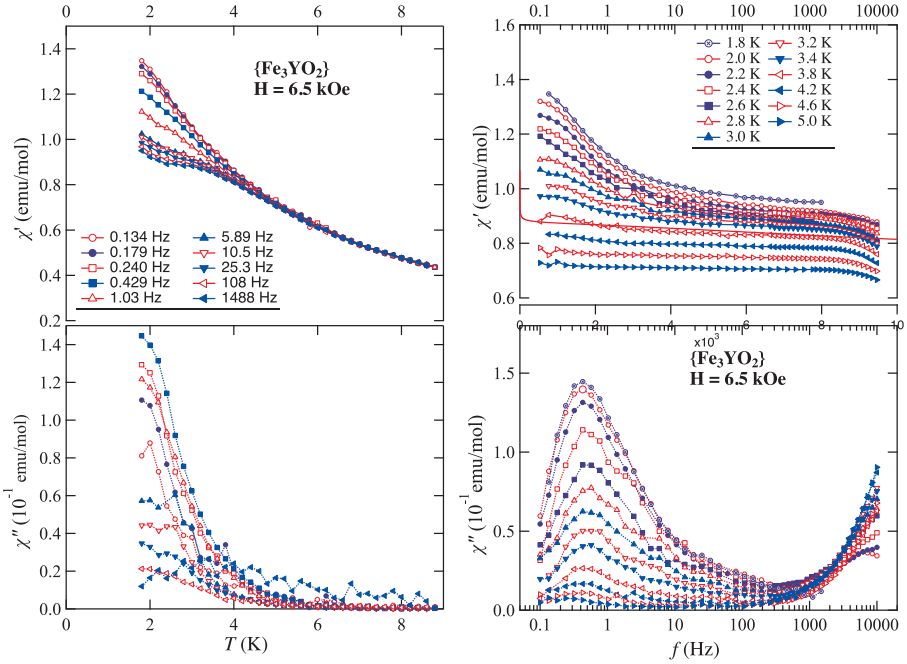

Fig. 7 Left panels: $\chi'(T)$ and $\chi''(T)$ at different frequencies and applied field $H = 6.5$ kOe for the $\{Fe_3YO_2\}$ compound. Right panels: $\chi'(f)$ and $\chi''(f)$ for temperatures from 1.8 to 5 K.

$M(H)$ curves,[37–41] although in most of the studied molecules the anisotropy parameter is positive, or there is no unambiguous determination of its sign. However, it should be recalled that only in the molecule studied by Solano-Peralta *et al.*[41] ($D_i/k_B = 0.28$ K) the Fe(III) ion is coordinated in an O_6 octahedron, while in the other cases the octahedral environment contains several nitrogen atoms. It is worth mentioning that the Schottky anomaly appearing in the heat capacity unambiguously allows to assign a sign to D, since its shape greatly depends on the sign of D. Indeed, since the separation between the $m = \pm 5/2$ and $m = \pm 3/2$ doublet states is $6D$, but that of $m = \pm 3/2$ and $m = \pm 1/2$ is $4D$, the levels scheme for negative D (ground state $m = \pm 5/2$) and positive D (ground state $m = \pm 1/2$) gives quite different heat capacity contribution.

The value of the Fe_3 cluster anisotropy constant $D/k_B = -0.56(3)$ K in the present Fe_3 cluster is in the range of those reported in other polynuclear iron clusters from different experimental techniques. In the $S = 5/2$ trinuclear Fe^{3+} magnetic cluster of $[Fe_3O(O_2CBut)_2(N_3)_3(dmem)_2]$, $D/k_B = -0.99$ K was derived from magnetic measurements .[42] In $S = 5$ tetranuclear Fe^{3+} molecular clusters, heat capacity and neutron inelastic scattering measurements on $Fe_4(OCH_3)_6(dpm)_6$ (H*dpm*=dipivaloylmethane) produced the value $D/k_B = -0.28(1)$ K,[43] while in $[Fe_4(thme)_2(dpm)_6]$ $D/k_B = -0.64$ K from HF-EPR spectra[44] and $D/k_B = -0.65$ K from inelastic neutron scattering spectra, albeit with a rhombic term $E/k_B = -0.014$ K.[45] In all these cases, as in $\{Fe_3YO_2\}$, the cluster has a negative effective D parameter, and therefore the lowest level is that of the highest quantum number $|m| = 5/2$.[21]

The intercluster interaction disclosed by the excess in entropy shown in the heat capacity measurements was modelled as antiferromagnetic chains. The *dc* magnetic susceptibility calculated with simple models and the anisotopy D and intercluster interaction J parameters obtained from the heat capacity data, is in qualitative agreement with the experimental results (Fig. 4). Since this type of "butterfly" molecule compounds were not expected to show magnetic single chain magnetic behaviour because of the structural distribution of its Fe_3 clusters, it is of interest to show how are the chains conformed where spin correlations are observed. The $\{Fe_3YO_2\}$ compound crystallizes in the monoclinic system (S.G. $P2_1$, $Z = 2$) with cell parameters $a = 13.0515(10)$ Å, $b = 14.5745(11)$ Å, $c = 20.0068(16)$ Å, and $\beta = 93.882(1)°$.[15] The simplified structure of Fe_3 clusters can be viewed as formed by two sets of Fe_3 clusters whose planes are at approximately 90° and the distances between centroids of clusters range from 11.85 Å to 20.01 Å (Fig. 8). The minimum intercluster distances depict a zig-zag line of Fe_3 clusters with alternating perpendicular cluster planes, and the next closest neighbour cluster centroids are at least at distances 10% larger. Perfect antiferromagnetic alignment is realized for anisotropy direction along $[hkl] \approx [101]$, which is a direction close to one on the Fe_3 planes and joining the "body" Fe(2) ion and the midpoint of the "wing-to-wing" Fe(1)-Fe(3) bond (Fig. 8). Second neighbour interactions along the crystallographic b axis or small deviations from the proposed anisotropy direction would give rise to a weak ferromagnetic component perpendicular to the antiferromagnetic spin correlations. This can produce a non-zero χT value at the low temperature limit, as experimentally observed (Fig. 2-bottom), although an additional effect arising from a not fully random easy axes orientation within the powder sample cannot be precluded.

View Article Online
DOI: 10.1039/C9DT04816B

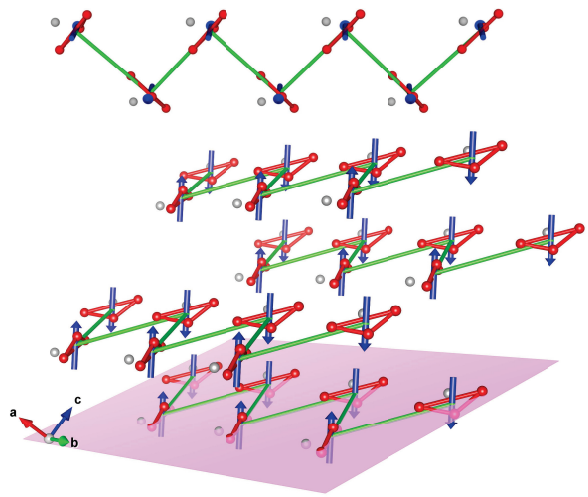

Fig. 8 Chain of Fe_3 clusters along a zig-zag line with minimum intercluster distance. Cluster magnetic moments are depicted by arrows along the anisotropy axis contained in the cluster's plain. Only the triangular Fe_3 clusters are shown along with lines connecting the cluster centroids in the antiferromagnetic chain; the rest of the atoms, except Y (faded), are hidden for sake of clarity. Bottom figure: the centroids of the Fe_3 clusters which compose the spin chains are contained in planes (one is depicted). Top figure: a single chain viewed from the top of its plane with antiferromagnetic coupling. The magnetic moments point out of and into the chain's plane.

The "fast" relaxation process observed in the *ac* susceptibility measured between 2 to 5 K shows an Arrhenius' type temperature dependence with an activation energy $E_a/k_B = 3.4(6)$ K. It is well known that the relaxation time in single chain magnets contains two additive contributions.[21,46,47] On the one hand, a thermally activated "single ion" (here, single Fe_3 cluster or single molecule) process over the anisotropy barrier (Orbach process). The energy barrier is $\Delta_A = |D|\left(S^2 - \frac{1}{4}\right)$ for a half-integer spin S with uniaxial anisotropy; this amounts to $\Delta_A/k_B = 3.36$ K in the present case. However, since the relaxation times were obtained with *ac* suscetibility with a *dc* magnetic field of $H = 6.5$ kOe, the three doublets of the $S = 5/2$ multiplet are split, which reduces in the single-molecule activation energy.[21] For a single crystal, the corrected activation energy is $\Delta'_A = \left[S - \frac{g\mu_B H_z}{2|D|}\right]^2$, where H_z is the magnetic field along the anisotropy axis.* Assuming a random powder sample under an applied field H, an average activation energy is obtained $\overline{\Delta'_A}/k_B = \frac{|D|}{k_B}\left[S^2 - S\frac{g\mu_B H}{2|D|} + \frac{1}{3}\left(\frac{g\mu_B H}{2|D|}\right)^2\right] \approx 2.52$ K, where H is the applied *dc* magnetic field.

On the other hand, the intercluster interaction in the chains produces domains of length 2ξ, with ξ the correlation length, which diverges at $T = 0$ since it is a 1D system. Relaxation in the chain reflects the thermal motion of domain walls. For $D/J > 4/3$ (J as defined in eq. 5), which is our case, domain walls are very narrow, the limit being a single spin and a domain wall energy $\Delta_\xi = 4JS^2 \approx 1$ K, hence likely to compete with single-molecule relaxation. The activation energy for the infinite chain is $2\Delta_\xi = 8JS^2$. However, defects in the structure limits the average length L of the chains and in the low temperature limit the correlation length can be so large that $2\xi > L$ (finite chain limit); in that situation the activation energy decreases to $\Delta_\xi = 4JS^2$. Consequently, the total activation energy (Δ_τ as obtained from the measured relaxation time τ) when no *dc* magnetic field is applied will be $\Delta = \Delta_A + 8JS^2$ or $\Delta = \Delta_A + 4JS^2$ ($\approx 3.5\,\text{K} < \Delta/k_B < 4.5\,\text{K}$) with a crossover depending on the temperature and defect concentration (determining the chain length L). In either case, the single molecule anisotropy activation energy Δ_A is expected to be increased by the chain correlations.

It should be stressed that the above account of the contributions of the chain correlations to the activation energy is valid for vanishing applied field. When a *dc* field is applied, as in the present *ac* susceptibility measurements, this field will affect the relaxation time and hence the total activation energy. For ferromagnetic chains, Coulon *et al.*[47,48] have modelled this effect in the framework of Glauber's theory of the 1D Ising model dynamics.[49] For finite chains they have found that the activation energy depends on the the probability law used and the relative strength of the applied field with respect to the domain wall energy, $h = \mu H/\Delta_\xi$ with $\mu = g\mu_B S$ the magnetic moment of the magnetic unit. The "probability law" is the function that represents the transition probability of a spin at a site in the chain to flip to its opposite direction while the others remain momentarily fixed. While Δ is independent of h for Glauber's probability law,[49] it decreases for other models as an external magnetic field is applied (see ESI†).[47] For the antiferromagnetic case, no similar calculations are available yet. However, we may note that finite antiferromagnetic Ising-like chains are expected to be fully polarized by the external *dc* field for $\mu H > |J|$[50] (*i.e* $h > 0.04$) and the relaxation behaviour can then be expected to be similar to that of ferromagnetic chains. In the present case, $h \approx 1$.

The present experimental activation energy $\Delta_\tau = 3.4(6)$ K is clearly accounted for by a single-molecule process with activation energy $\overline{\Delta'_A}/k_B = 2.51$ K under the external applied magnetic field $H = 6.5$ kOe plus chain correlations with activation energy $4JS^2/k_B \approx 1$ K unaffected by the field, which points to Glauber's probability law as governing the relaxation process.

6 Conclusions

The present work shows that the heat capacity and *dc* susceptibility of the butterfly molecules compounds $\{Fe_3YO_2\}$ allow to give a good estimation of the ligand field anisotropy constant as well as its sign for polynuclear iron clusters with effective spin value $S_{Fe3} = 5/2$. Additionally intercluster interactions that are realized as an antiferromagnetic single chain magnet system are disclosed. The chain interaction constant J is an order of magnitude smaller than the single ion uniaxial anisotropy constant D.

At very low temperature, temperature indenpendent quantum tunneling of the magnetization of the magnetic moment of the

* This result is the same for integer and half integer spin.

View Article Online
DOI: 10.1039/C9DT04816B

Fe_3 clusters is observed. In a slightly higher temperature range, a relaxation process with an exponential temperature dependence and relaxation times of the order of 10^{-5} s is revealed by applying an external *dc* magnetic field on the *ac* susceptibility measurements. The applied magnetic field affects the measured relaxation times, which is reflected in the single-molecule activation energy. However the chain intercluster relaxation process is not affected by this applied magnetic field pointing to Glauber's probability law as the one describing spin flips in this single chain magnetic system. Therefore, the present example contributes to explore the properties of single chain magnets in the narrow wall limit ($D/J > 4/3$) with "high *dc* field", where very few results are still available.[47]

Acknowledgments

We acknowledge financial support from the MICNN projects MAT2017-83468-R, RTI2018-096075-B-C21 and PCI2018-093116, as well as COST Action on Molecular Spintronics (CA15128, MOLSPIN). The authors would like to acknowledge the use of the Servicio General de Apoyo a la Investigación-SAI, Universidad de Zaragoza, and Aragonese E12_17R RASMIA and E09_17R Q-MAD (co-funded by Fondo Social Europeo), and of the European Union FEDER (ES).

Notes and references

1 E. Burzurí and H. van der Zaant, *Molecular magnets: Physics and Applications*, Springer, Berlin, 2014, pp. 297–318.
2 M. N. Leuenberger and D. Loss, *Nature*, 2001, **410**, 789–793.
3 M. Affronte and F. Troiani, *Molecular Magnets. Physics and Applications*, Springer, Berlin, 2014, pp. 249–273.
4 K. v. Hoogdalem, D. Stepanenko and D. Loos, *Molecular Magnets. Physics and Applications*, Springer, Berlin, 2014, pp. 275–296.
5 M. Mannini, F. Pineider, C. Danieli, F. Totti, L. Sorace, P. Sainctavit, M. Arrio, E. Otero, L. Joly, J. C. Cezar, A. Cornia and R. Sessoli, *Nature*, 2010, **468**, 417–421.
6 M. D. Jenkins, D. Zueco, O. Roubeau, G. Aromí, J. Majer and F. Luis, *Dalton Trans.*, 2016, **45**, 16682–16693.
7 M. Evangelisti, *Molecular Magnets. Physics and Applications*, Springer, Berlin, 2014, pp. 365–387.
8 N. V. Prokof'ev and P. C. E. Stamp, *Phys. Rev. Lett.*, 1998, **80**, 5794–5797.
9 J. J. Alonso and J. F. Fernández, *Phys. Rev. Lett.*, 2001, **87**, 097205.
10 F. L. J. Campo, J. Gómez, G. McIntyre, J. Luzón and D. Ruiz-Molina, *Phys. Rev. Lett.*, 2005, **95**, 227202.
11 E. Burzurí, F. Luis, B. Barbara, R. Ballou, E. Ressouche, O. Montero, J. Campo and S. Maegawa, *Phys. Rev. Lett.*, 2011, **107**, 097203.
12 J. Bartolomé, G. Filoti, V. Kuncser, G. Schinteie, V. Mereacre, C. E. Anson, A. K. Powell, D. Prodius and C. Turta, *Phys. Rev. B*, 2009, **80**, 014430.
13 J. Luzón and R. Sessoli, *Dalton Trans.*, 2012, **41**, 13556.
14 J. Tang, I. Hewitt, N. T. Madhu, G. Chastanet, W. Wernsdorfer, C. E. Anson, C. Benelli, R. Sessoli and A. K. Powell, *Angew. Chemie - Int. Ed.*, 2006, **45**, 1729–1733.
15 V. Mereacre, D. Prodius, C. Turta, S. Shova, G. Filoti, J. Bartolomé, R. Clérac, C. E. Anson and A. K. Powell, *Polyhedron*, 2009, **28**, 3017–3025.
16 L. Badía-Romano, F. Bartolomé, J. Bartolomé, J. Luzón, D. Prodius, C. Turta, V. Mereacre, F. Wilhelm and A. Rogalev, *Phys. Rev. B*, 2013, **87**, 184403.
17 L. Badía-Romano, J. Rubín, F. Bartolomé, J. Bartolomé, J. Luzón, D. Prodius, C. Turta, V. Mereacre, F. Wilhelm and A. Rogalev, *Phys. Rev. B*, 2015, **92**, 064411.
18 L. Badía-Romano, J. Rubín, F. Bartolomé, J. Bartolomé, J. Luzón, D. Prodius, C. Turta, V. Mereacre, F. Wilhelm and A. Rogalev, *J. Magn. Magn. Mater.*, 2016, **400**, 137–140.
19 C. Turta, D. Prodius, V. Mereacre, S. Shova, M. Gdaniec, Y. Simonov, V. Kuncser, G. Filoti, A. Caneschi and L. Sorace, *Inorg. Chem. Commun.*, 2004, **7**, 576–579.
20 E. S. R. Gopal, *Specific Heats at Low Temperatures*, Heywood Books, London, 1966.
21 D. Gatteschi, R. Sessoli and J. Villain, *Molecular Nanomagnets*, University Press, Oxford, 2006.
22 J. Borrás-Almenar, J. Clemente-Juan, E. Coronado and B. Tsukerblat, *Inorg. Chem.*, 1999, **38**, 6088.
23 B. M. McCoy and T. T. Wu, *The Two Dimensional Ising Model*, Harvard University Press, Cambridge, Massachusetts, 1973.
24 M. Lines, *Phys. Rev. Lett.*, 1979, **42**, 533–536.
25 H. W. Capel, *Physyca*, 1966, **32**, 966–988.
26 I. Chatterjee, *J. Math. Phys.*, 1985, **25**, 2339–2344.
27 B. Frank and M. Elofer, *J. Stat. Phys.*, 1987, **46**, 559–565.
28 P. Asselin, R. F. L. Evans, J. Barker, R. W. Chantrell, R. Yanes, O. Chubykalo-Fesenko, D. Hinzke and U. Nowak, *Phys. Rev. B*, 2010, **82**, 054415.
29 J. H. van Vleck, *Phys. Rev.*, 1940, **57**, 426–447.
30 B. Abragam and B. Bleaney, *Electron Paramagnetic Resonance of Transition Ions*, Dover, 1970.
31 K. S. Cole and R. H. Cole, *J. Chem. Phys.*, 1941, **9**, 341–351.
32 E. Bartolomé, J. Bartolomé, S. Melnic, D. Prodius, S. Shova, A. Arauzo, J. Luzón, F. Luis and C. Turta, *Dalton Trans.*, 2013, **42**, 10153–10171.
33 A. Arauzo, A. Lazarescu, S. Shova, E. Bartolomé, R. Cases, J. Luzón, J. Bartolomé and C. Turta, *Dalton Trans.*, 2014, **43**, 12342–12356.
34 E. Bartolomé, J. Bartolomé, S. Melnic, D. Prodius, S. Shova, A. Arauzo, J. Luzón, L. Badía-Romano, F. Luis and C. Turta, *Dalton Trans.*, 2014, **43**, 10999–11013.
35 E. Bartolomé, J. Bartolomé, A. Arauzo, J. Luzón, L. Badía, R. Cases, F. Luis, S. Melnic, D. Prodius, S. Shova, and C. Turta, *J. Mater. Chem. C*, 2016, **4**, 5038–5050.
36 A. Bencini and D. Gatteschi, *Electron Paramagentic Resonance of Exchange Coupled Systems*, Springer-Verlag, Berlin Heidelberg, 1990.
37 R. Herchel, L. Pavelek and Z. Trávníček, *Dalton Trans.*, 2011, **40**, 11896.
38 I. Nemec, R. Boča, M. Gembický, L. Dlháň, R. Herchel and F. Renz, *Inorg. Chim. Acta*, 2009, **362**, 4754–4759.

View Article Online
DOI: 10.1039/C9DT04816B

39 R. Hernández-Molina, A. Mederos, S. Domínguez, P. Gili, C. Ruíz-Pérez, A. Castiñeiras, X. Solans, F. Lloret and J. A. Real, *Inorg. Chem.*, 1998, **37**, 5102–5108.

40 R. Ishikawa, B. K. Breedlove and M. Yamashita, *Eur. J. Inorg. Chem.*, 2013, **2**, 716–719.

41 A. Solano-Peralta, J. P. Saucedo-Vázquez, R. Escudero, H. Höpfl, H. El-Mkami, G. M. Smith and M. E. Sosa-Torres, *Dalton Trans.*, 2009, **9**, 1668–1674.

42 R. Bagai, S. Datta, A. Betancur-Rodriguez, K. a. Abboud, S. Hill and G. Christou, *Inorg. Chem.*, 2007, **46**, 4535–4547.

43 G. Amoretti, S. Carretta, R. Caciuffo, H. Casalta, A. Cornia, M. Affronte and D. Gatteschi, *Phys. Rev. B*, 2001, **64**, 1–7.

44 A. Cornia, A. C. Fabretti, P. Garrisi, C. Mortalò, D. Bonnachi, D. Gatteschi, R. Sessoli, L. Sorace and W. Wernsdorfer, *Angew. Chem. Int. Ed. Engl.*, 2004, **43**, 1136.

45 S. Carretta, P. Santini, G. Amoretti, T. Guidi, R. Caciuffo, A. Candini, A. Cornia, D. Gatteschi, M. Plazanet and J. A. Stride, *Phys. Rev. B*, 2004, **79**, 214403.

46 C. Coulon, H. Miyasak and R. Clérac, *Single-Molecular Magnets and Related Phenomena*, Springer-Verlag, Berlin Heidelberg, 2006, vol. 122, pp. 163–206.

47 C. Coulon, V. Pianet, M. Urdampilleta and R. Clérac, *Molecular Nanomagnets and Related Phenomena*, Springer-Verlag, Berlin Heidelberg, 2015, vol. 164, pp. 143–184.

48 C. Coulon, R. Clérac, W. Wernsdorfer, T. Colin, A. Saitoh, N. Motokawa and H. Miyasaka, *Phys. Rev. B*, 2007, **76**, 214422.

49 R. Glauber, *J. Math. Phys.*, 1963, **4**, 294–307.

50 F. Matsubara, K. Koshimura and S. Katsura, *Can. J. Phys.*, 1973, **51**, 1053–1063.

View Article Online
DOI: 10.1039/C9DT04816B

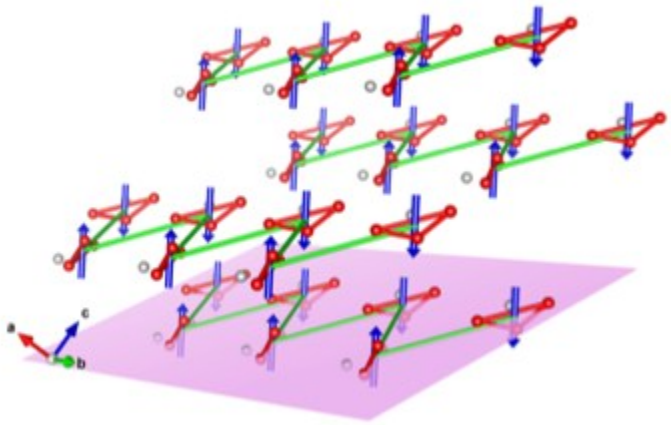

Supramolecular magnetic chains of Fe_3 clusters in a molecular complex.